RSC Advances

ROYAL SOCIETY OF CHEMISTRY

www.rsc.org/advances

Cite this: DOI: 10.1039/c0xx00000x

www.rsc.org/xxxxxx

ARTICLE TYPE

Facile synthesis of nanocomposite based on graphene and ZnAl layered double hydroxides as a portable shelf of luminescent sensor for DNA detection

Hongjuan Li,*[a] Jia Wen,[a] Ruijin Yu,[a] Jia Meng,[a] Cong Wang,[a] Chaoxia Wang[b] and Shiguo Sun*[a]

Received (in XXX, XXX) Xth XXXXXXXXX 20XX, Accepted Xth XXXXXXXXX 20XX
DOI: 10.1039/b000000x

Recently, nanocomposites based on graphene and layered double hydroxides (LDH) have been developed and used in many fields. However, to our knowledge, there is no report on the luminescence sensor applications of graphene/LDH composites. Herein, a hybrid graphene/ZnAl-LDH nanocomposite has been developed using a facile one-step process and the presence of LDH in the composite can effectively prevent the restacking of graphene and improve both the luminescence properties and thermal stability. Furthermore, the composite can be used as a portable shelf of the $Ru(phen)_3Cl_2$ (tris(1,10-phenanthroline)ruthenium(II) dichloride) sensor to selective discriminate DNA. It is found that the graphene/ZnAl-LDH composite can effectively quench the emission of the $Ru(phen)_3Cl_2$ sensor. After the addition of a certain amount of DNA into the system, $Ru(phen)_3Cl_2$ was released from graphene/ZnAl-LDH composite and interacted with DNA immediately, leading to a luminescence recovery of the sensor. The results indicate that the RGO/ZnAl-LDH composite displayed an excellent luminescence response and good linear correlation to DNA. So the composite can be employed as a portable shelf of $Ru(phen)_3Cl_2$ to discriminate DNA. And both the shelf and the sensor can be easily collected and ready for the next sample if there is not any DNA existed in the solution. The proposed method was further applied to detect the immunodeficiency virus gene (HIV), providing a new field of application of the hybrid graphene/LDH composite.

Introduction

Graphene, a two-dimensional monolayer carbon material, have been widely researched because of its large specific surface area, high electrical/thermal conductivity, high flexibility, and unusual mechanical strength, etc.[1-3] However, the restacking of graphene sheets during the reduction and drying processes has severely hampered the performance of graphene materials.[4-5] Functionalization of graphene has been widely regarded as an efficent way to improve the dispersibility and stability.[6] Due to the ease of chemical modification, high surface area, electrical conductivity and high flexibility, graphene could assembly with other functional nanomaterials to form the hybrid graphene-based nanocomposites.[7] Owing to their unique nanostructure, high specific surface area and good biocompatibility, graphene-based nanocomposites have shown potential applications in the field of biological/chemical sensors, cellular imaging, drug delivery, and so on.[8-13] According to research, the presence of other functional nanomaterials in the graphene-based composites can not only effectively prevent the agglomeration and restacking of graphene but also improve the dispersibility, stability and some properties of materials.[14-15]

Layered double hydroxides (LDH) materials can be a good candidate of this kind of nanomaterials. Up to now, Some LDH materials (such as MgAl-LDH, ZnAl-LDH) have shown prospective application in biological field, due to their high biocompatibility, low cytotoxicity, low cost, opened layer structure, high anion exchange capacity.[16-22] In recent years, nanocomposites based on graphene and LDH materials have been developed, which were used as supercapacitors, Li-ion batteries, catalysts, photocatalysis, heavy metal removal, and so on.[23-30] However, to our knowledge, there is no report on the luminescence sensor applications of graphene/LDH composite.

Herein, a hybrid graphene/ZnAl-LDH composite was developed using a simple and green approach. In the synthesis procedure, the exfoliated graphite oxide (GO) is simultaneously reduced to graphene in company with the homogeneous precipitation of ZnAl-LDH to form a hybrid graphene/ZnAl-LDH composite. The as-prepared graphene nanocomposite was found to effectively quench the emission of $Ru(phen)_3Cl_2$ (tris(1,10-phenanthroline)ruthenium(II) dichloride), a DNA sensor in aqueous solution. After being encountered with CT DNA, $Ru(phen)_3Cl_2$ was released from RGO/ZnAl-LDH composite and interacted with CT DNA immediately, leading to a luminescence recovery of $Ru(phen)_3Cl_2$. The luminescence increase is linearly proportional to the amount of DNA added, demonstrating that the composite can be employed as a portable shelf of $Ru(phen)_3Cl_2$ to selective discriminate DNA. If there is not any DNA existed in the solution, both the shelf and the sensor can be easily collected and ready for the next sample, the proposed method was further applied to detect the immunodeficiency virus gene (HIV), providing a new field of application for the hybrid graphene/ZnAl-LDH composite.

Experimental

Materials

All the chemicals are of analytical grade and were used without further purification. Natural flake graphite (325 mesh) was purchased from Alfa-Aesar Co. Calf thymus DNA (CT DNA), bovine serum albumin (BSA), pepsin, thrombin, casein, RNase myoglobin and concanavalin were purchased from Sigma Chemical Co. Ultrapure Milli-Q water (ρ>18.0 MΩ cm) was used throughout the fluorescence experiments. The ruthenium(II) complexes ($Ru(phen)_3Cl_2$) used in experiments were synthesized according to the literature procedure.[31] The immunodeficiency virus gene (HIV) was synthesized by Beijing AuGCT DNA-SYN Biotechnology Co., Ltd. And the sequences of the oligonucleotides were listed as follows:

Target DNA:
5′-ATCCCATTCTGCAGCTTCCTCATTGATGGTCTC-3′
Probe DNA:
5-GAGACCATCAATGAGGAAGCTGCAGAATGGGAT-3′

Preparation of the graphene/ZnAl-LDH nanocomposite

Graphite oxide (GO) was synthesized from natural flake graphite by a modified Hummers method.[32] Graphene/ZnAl-LDH composite was prepared via a solution approach. In a typical procedure, the as-prepared GO (100 mg) was dispersed in deionized water (500 mL) with the assistance of sonication for 60 min. Subsequently, $ZnCl_2$, $AlCl_3{\cdot}6H_2O$ and urea were added into the above suspension to give the final concentration of 10, 5 and 35 mM, respectively. After being vigorously shaken for a few minutes, the suspension was then refluxed at 100 ºC for 24 h under continuous magnetic stirring. The resulting black product was filtered, washed with deionized water, and dried in air, which was abbreviated as RGO/ZnAl-LDH. Herein urea was used as a hydrolysis agent to adjust pH value and also as a reductant to reduce GO into graphene.

For comparison, pure ZnAl-LDH was also prepared in the same procedure using $ZnCl_2$, $AlCl_3{\cdot}6H_2O$ and urea but without GO. To prepare graphene, only the exfoliated GO suspension (0.2 mg/mL, 500 mL) was refluxed at 100 ºC for 24 h in the presence of urea (35 mM) under the same experimental condition. The resulting product was abbreviated as RGO.

Characterization

X-ray diffraction (XRD) analysis was carried out with a D/Max2550VB+/PC X-ray diffractometer with Cu Kα (λ =0.15406 nm), using an operation voltage and current of 40 kV and 30 mA, respectively. A Quanta 200 environmental scanning electron microscopy (SEM) was used to observe the morphologies of the obtained materials. Transmission electron microscopy (TEM) images were collected using a JEM-2100 microscope working at 200 kV. Specimens for observation were prepared by dispersing the samples into alcohol by ultrasonic treatment and dropped on carbon–copper grids. The X-ray photoelectron spectroscopy (XPS) measurement was performed with an Axis Ultra, kratos (UK) spectrometer using Al Kα excitation radiation (1486 eV). Thermogravimetry analysis (TGA) was obtained on a thermal analyzer (Q1000DSC + LNCS + FACS Q600SDT) under air atmosphere at a heating rate of 10 °C min^{-1}. The absorption and emission spectra were collected using a Shimadzu 1750 UV-visible spectrometer and a RF-5301 fluorescence spectrometer (Japan), respectively.

2.4. Luminescence experiments

Stock of CT DNA was prepared by dissolving commercial CT DNA in ultrapure water. The concentration of CT DNA was determined spectrophotometrically. Stock solution of $Ru(phen)_3Cl_2$ (0.49 μM) was prepared in ultrapure water. The RGO/ZnAl-LDH composite was added in ultrapure water and sonicated for 2 h until the composite dispersed homogeneously in solution (50 mg/mL). Then the above RGO/ZnAl-LDH composite suspension was gradually added into $Ru(phen)_3Cl_2$ solution (3 mL) with stirring until the luminescence was almost quenched. Finally, an increasing amount of CT DNA solution was added until the highest luminescence intensity was reached. The sample was stirred for 5 s each time, and the supernatant was determined by fluorescence spectrophotometer. In all the titration experiments, the total volume was maintained not exceed 5% of the original volume.

3. Results and discussion

X-ray diffraction analysis

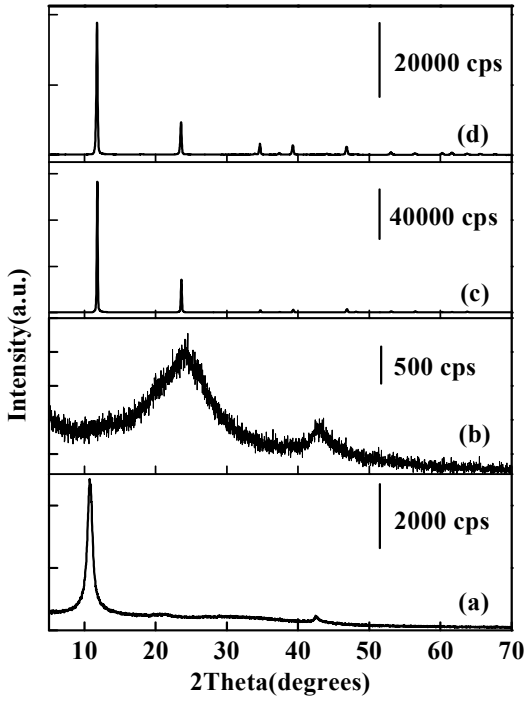

Fig. 1 XRD patterns of (a) GO, (b) RGO, (c) pure ZnAl-LDH, and (d) RGO/ZnAl-LDH composite.

The X-ray diffraction (XRD) patterns of the prepared GO, pure ZnAl-LDH, RGO and the as-prepared RGO/ZnAl-LDH composite are presented in Fig. 1. The XRD pattern of the GO (Fig. 1a) exhibits a reflection peak at 2θ = 10.7° with an interlayer spacing of 0.82 nm, confirming the formation of graphite oxide.[33] After its reduction with urea, the peak at 10.7° of GO completely disappears (Fig. 1b) and only a abroad diffraction peak at around 24.4° is observed, corresponding to the C(002) reflection of graphene. The result suggests that GO was reduced to graphene after treating with urea. The XRD pattern of

pure ZnAl-LDH (Fig. 1c) shows an obvious layered structure with a basal spacing of 0.75 nm, which is in good agreement with the characteristic peaks of the standard compound $Zn_{0.63}Al_{0.37}(OH)_2(CO_3)_{0.185}\cdot x(H_2O)$ (JCPDS: 48-1024).[34] The XRD pattern of the as-prepared RGO/ZnAl-LDH composite shows that the diffraction peaks are similar to those of the pristine ZnAl-LDH (Fig. 1d). The diffraction peaks of graphene are not distinguishable in the composite, implying that GO has reduced into graphene in the presence of urea[35] and the restacking of the as-reduced graphene sheets is effectively prevented by the introduction of ZnAl-LDH, which results in the shielding of the graphene peaks by those of ZnAl-LDH.[36-37] This result suggests that in company with the homogeneously precipitation of ZnAl-LDH platelets on the surface of GO nanosheets, GO nanosheets are simultaneously reduced into graphene to form the hybrid graphene/ZnAl-LDH composite.

X-ray photoelectron spectroscopy analysis

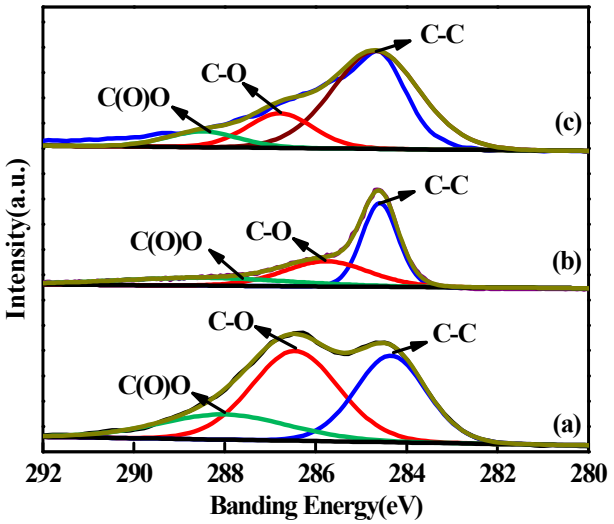

Fig. 2 C1s XPS spectra of (a) GO, (b) RGO, and (c) RGO/ZnAl-LDH composite.

The reduction of GO can be further confirmed by X-ray photoelectron spectroscopy (XPS) analysis presented in Fig. 2. The C1s spectrum of GO shows three types of carbon bonds as shown in Fig. 2a. The peak of the non-oxygenated ring C (C–C) located at 284.4 eV is assigned to bonds between sp^2 hybridized carbon atoms. And two peaks at 286.5 and 288.0 eV are attributed to epoxy and alkoxy carbon (C–O) and the carboxylate carbon (O–C = O), indicating a considerable degree of oxidation.[38-39] The C1s XPS spectrum of RGO (Fig. 2b) and RGO/ZnAl-LDH composite (Fig. 2c) also exhibits these three types of carbon. However, compared to that of GO, the absorbance band intensities of the epoxy and alkoxy carbon (C–O) and the carboxylate carbon (O–C = O) of RGO and RGO/ZnAl-LDH composite decrease significantly due to the reduction of GO to graphene. By integrating the area of these peaks, the percentage of oxygen-containing ring C in the GO is calculated to be 64 %, while that of the RGO/ZnAl-LDH composite is 28 %. These results indicate that most of the oxygen-containing functional groups in RGO/ZnAl-LDH composite are removed, confirming a successful reduction of GO to graphene. For the sample of RGO in the control experiment, the percentage of oxygenated ring C is calculated to be 48 %, which is higher than that of RGO/ZnAl-LDH composite. These results indicate that by adding ZnAl-LDH in the composite can lead to RGO/ZnAl-LDH nanocomposite with RGO in a higher reductive degree. This result can be explained that the restacking of the as-reduced graphene sheets is effectively prevented by the introduction of ZnAl-LDH, which is consistent with the XRD analysis. The XPS wide scan spectrum of RGO/ZnAl-LDH composite (Fig. S1) not only exhibits the peaks of O1s and C1s, but also exhibits the peaks of Zn 2p and Al 2p, suggesting the formation of RGO/ZnAl-LDH composite.

Surface morphology and thermogravmetric analysis

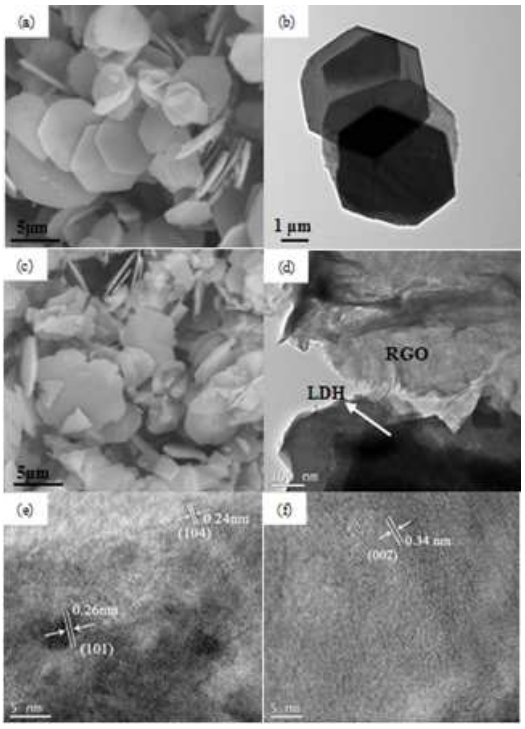

Fig. 3 (a) SEM and (b) TEM images of ZnAl-LDH. (c) SEM and (d) TEM images of RGO/ZnAl-LDH composite. (e), (f) high-resolution TEM images of RGO/ZnAl-LDH composite.

SEM and TEM images of pure ZnAl-LDH and the as-prepared RGO/ZnAl-LDH composite are presented in Fig. 3. It is seen that the pure ZnAl-LDH material is consisted of thin hexagonal platelets with a mean lateral size of about 5 μm (Fig. 3a, 3b). In contrast, SEM and TEM images (Fig. 3c, 3d) of the RGO/ZnAl-LDH composite exhibit both relative irregular hexagonal platelets of ZnAl-LDH and the corrugation and scrolling image of graphene nanosheets. The result indicates that ZnAl-LDH platelets are grown on the surface of graphene nanosheets to form the RGO/ZnAl-LDH composite during the urea reflux procedure. From the HRTEM image of the RGO/ZnAl-LDH composite (Fig. 3e, 3f), three kinds of contrast fringes can be observed. The lattice fringe with an interplanar distance of 0.34 nm is in accordance with that of the graphite (002) plane.[40] And the lattice fringes with an interplanar distance of 0.24 and 0.26 nm are ascribed to the (104) and (101) plane of the hexagonal ZnAl-LDH phase.[41] Since the introduction of ZnAl-LDH nanosheets, the

restacking of graphene nanosheets can be effectively prevented, which is consistent with the XRD results.

The thermal behaviors of RGO and the hybrid RGO/ZnAl-LDH composite are investigated by thermogravmetric analysis (TGA) in dry air. As shown in Fig. S2a, RGO prepared in the control experiment undergoes a consecutive weight loss of 90 %, which corresponds to the release of adsorbed water and the combustion of the carbon skeleton.[42] While the RGO/ZnAl-LDH composite (Fig. S2b) exhibits three-step weight loss of only 31 %, attributing to the release of the interlayer water, the dehydroxylation of ZnAl-LDH nanolayers in the hybrid RGO–Ni–Fe LDH material, and the combustion of the carbon skeleton, respectively.[43] However, the residue percentage of the RGO/ZnAl-LDH composite (69 %) is much higher than that of RGO (10 %), suggesting that the combination of ZnAl-LDH with graphene significantly improves the thermal stability.

Luminescence spectra analysis

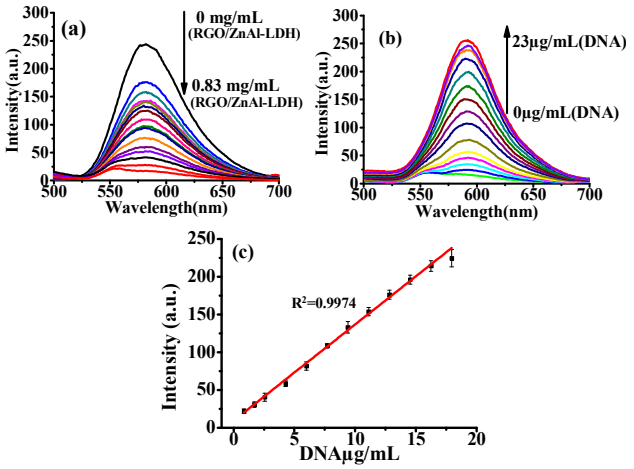

Fig. 4 Luminescence spectra of $Ru(phen)_3Cl_2$ in aqueous solution (a) upon addition of different concentration of RGO/ZnAl-LDH composite; (b) upon addition of different concentration of CT DNA in the presence of 0.83 mg/mL RGO/ZnAl-LDH composite; (c) Luminescence signaling change at 592 nm plotted as the function of CTDNA concentation, Ex=464 nm.

The luminescence spectra of $Ru(phen)_3Cl_2$ (0.49 μM) in aqueous solution upon addition of different concentrations of RGO/ZnAl-LDH composite are shown in Fig. 4a. When RGO/ZnAl-LDH composite was added gradually into $Ru(phen)_3Cl_2$ in aqueous solution, the luminescence intensity of $Ru(phen)_3Cl_2$ decreases as RGO/ZnAl-LDH composite concentration increased, suggesting that strong π-π stacking interaction and electrostatic interaction existed between RGO/ZnAl-LDH composite and $Ru(phen)_3Cl_2$. When the concentration of RGO/ZnAl-LDH composite increases to 0.83 mg/mL, the luminescence intensity of $Ru(phen)_3Cl_2$ doesn't change any further. This means that no free $Ru(phen)_3Cl_2$ is left in the solution at this point. Then CT DNA was added gradually into the above mentioned solution. Along with the addition of CT DNA, the luminescence intensity was increased gradually as shown in Fig. 4b. This process can be explained as follows: After being encountered with CT DNA, $Ru(phen)_3Cl_2$ was released from RGO/ZnAl-LDH composite and interacted with CT DNA immediately, leading to a luminescence recovery of $Ru(phen)_3Cl_2$.[44-47] After 23 μg/mL DNA was added into the system, more than 17 times luminescence increase was observed. While, only 2 times luminescence increase was followed in the control experiment for $Ru(phen)_3Cl_2$ alone (Fig. S3).

As shown in Fig. 4c, the luminescence intensity was linearly related to the CT DNA added in the amount range from 0.8 to 18.0 μg/mL, with a correlation coefficient of 0.9974. The detection limit ($3\sigma/k$ method)[48] was 5.9 $\times 10^{-8}$ g/mL. It indicates that the hybrid RGO/ZnAl-LDH composite can be employed as a portable shelf of $Ru(phen)_3Cl_2$ to selective discriminate DNA.

To assess the selectivity of the detection, different proteins such as BSA, pepsin, thrombin, casein, myoglobin and concanavalin were measured. Firstly, the luminescence of $Ru(phen)_3Cl_2$ (0.49 μM) was fully quenched by RGO/ZnAl-LDH composite (0.83 mg/mL), then excess of various proteins were added separately into the cuvettes. The Luminescence response of $Ru(phen)_3Cl_2$ after addition excess of various proteins in the presence of RGO/ZnAl-LDH composite are shown in Fig. S4. The highest luminescence enhancement was observed only in the presence of CT DNA, while relative little change can be observed in the presence of the other proteins. It is noted that a small red shift of luminescence was found upon adding of CT DNA, whereas with adding of various proteins the luminescence peak undergoes a blue shift. The result thus demonstrated that this method had a high selectivity for CT DNA detection.

In order to investigate the role of Zn-Al layered double hydroxides in RGO/ZnAl-LDH composite for DNA detection. A comparison between RGO/ZnAl-LDH composite and RGO as well as Zn-Al LDH alone have been made through luminescence experiments as shown in Fig. S5. Luminescence spectra of $Ru(phen)_3Cl_2$ upon addition of different concentration of pure ZnAl-LDH and RGO are shown in Fig. S5a and S5b, respectively. When pure ZnAl-LDH were added gradually into $Ru(phen)_3Cl_2$ in aqueous solution, not much luminescence quenching can be observed, suggesting that almost no interaction existed between ZnAl-LDH and $Ru(phen)_3Cl_2$ (Fig. S5a). While for the sample of RGO in the control experiment, the luminescence intensity of $Ru(phen)_3Cl_2$ systematically decreases as the RGO concentration increased (Fig. S5b), suggesting that strong interaction existed between RGO and $Ru(phen)_3Cl_2$. Luminescence spectrum of $Ru(phen)_3Cl_2$ upon addition of different concentration of DNA in the presence of 5.7 μg/mL RGO is shown in Fig. S5c. As shown in Fig. S5c, after the addition of a certain amount of DNA, the luminescence intensity of RGO was increased by only 5-fold, which is lower than that of RGO/ZnAl-LDH composite (17 times increasing as shown in Fig. 4b). As shown in Fig. S5d, for the sample of RGO, the luminescence response shows a linear correlation to the DNA added over quite narrow concentration range from 0.04 to 0.38 μg/mL. The results indicate that RGO/ZnAl-LDH composite displayed a more excellent luminescence response, wide concentration range and good linear correlation to DNA than that of RGO and pure ZnAl-LDH. And the participation of ZnAl-LDH in the graphene composite can be helpful to effectively improve the luminescence properties.

The RGO/ZnAl-LDH composite was also employed as a portable shelf of $Ru(phen)_3Cl_2$ to discriminate the immunodeficiency virus gene (HIV) as shown in Fig. S6. When 0.3 mg/mL RGO/ZnAl-LDH composite was added into $Ru(phen)_3Cl_2$ in aqueous

solution, the luminescence intensity of $Ru(phen)_3Cl_2$ can be effectively quenched (Fig. S6a). Fig. S6b depicts the fluorescence spectra of $Ru(phen)_3Cl_2$ upon analyzing different concentrations of HIV target gene in the presence of 0.30 mg/mL RGO/ZnAl-LDH composite. As the concentration of the HIV gene increases, the resulting fluorescence is intensified. As shown in Fig. S6c, the luminescence intensity was linearly related to the HIV target gene added, indicating that the hybrid RGO/ZnAl-LDH composite can be also employed as a portable shelf of $Ru(phen)_3Cl_2$ to selective discriminate immunodeficiency virus gene (HIV).

On the basis of the above results, a schematic representation of the formation process of the RGO/ZnAl-LDH composite and the luminescence detection of DNA using the composite as a portable shelf of $Ru(phen)_3Cl_2$ is given in Fig. 5. GO, has a layered structure with a basal spacing of 0.82 nm, was first synthesized from graphite by a modified Hummers technique. Since there are different types of oxygen-containing functional groups (–OH, –COOH, C–O, etc.) on the surface of GO. When the exfoliated GO is soaked in a mixed solution of $ZnCl_2$, $AlCl_3•6H_2O$ and urea, positive Zn^{2+} and Al^{3+} ions can attach to the negatively charged functional groups on GO by electrostatic attraction and serve as nucleation precursors. In the urea refluxing process, a mass of nuclei form and the as-prepared ZnAl-LDH crystallites in situ grow and adhere to the surface of GO via an intermolecular hydrogen bond or a covalent coordination area, and meanwhile, GO is reduced to graphene in the existence of urea. The as-prepared RGO/ZnAl-LDH composite was found to effectively quench the emission of $Ru(phen)_3Cl_2$ due to strong π-π stacking interaction and electrostatic interaction existed between $Ru(phen)_3Cl_2$ and RGO/ZnAl-LDH composite. After being encountered with CT DNA, $Ru(phen)_3Cl_2$ was released from RGO/ZnAl-LDH composite and interacted with CT DNA immediately, leading to a luminescence recovery of $Ru(phen)_3Cl_2$. It is found that the luminescence increase is linearly proportional to the amount of DNA added. The composite can be employed as a portable shelf of $Ru(phen)_3Cl_2$ to selective discriminate DNA. If there is not any DNA existed in the solution, both the shelf and the sensor can be easily collected and ready for the next sample, providing some application into the hybrid graphene/LDH composite.

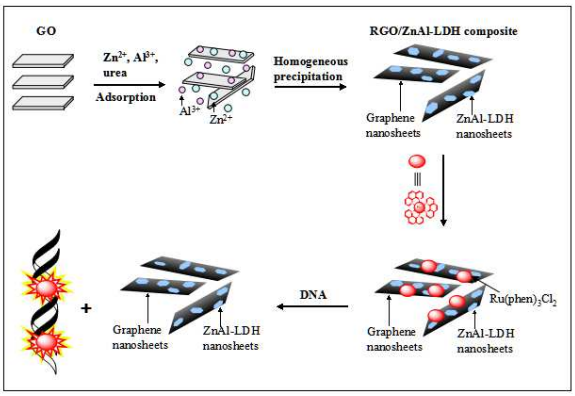

Fig. 5 Schematic representation of the formation process of RGO/ZnAl-LDH composite and the luminescence detection of DNA using the composite.

Conclusions

A hybrid RGO/ZnAl-LDH nanocomposite has been developed using a facile and green one-step process and used as a portable shelf of $Ru(phen)_3Cl_2$ sensor to selectively discriminate DNA. In the synthesis procedure, the exfoliated GO is simultaneously reduced to graphene using urea as the reductant in company with the homogeneous precipitation of ZnAl-LDH to form a hybrid graphene/ZnAl-LDH composite. The as-prepared RGO/ZnAl-LDH composite was found to effectively quench the emission of $Ru(phen)_3Cl_2$ in aqueous solution. A luminescence enhancement of approximately more than 17 times can be observed after addition of a certain amount of DNA into the above-mentioned system. Meanwhile, it is found that the luminescence increase is linearly proportional to the amount of DNA added in the concentration range of 0.8 to 18.0 μg/mL, with a correlation coefficient of 0.9974. The detection limit is 5.9×10^{-8} g/mL. So the composite can be employed as a portable shelf of $Ru(phen)_3Cl_2$ sensor to selectively discriminate DNA. Furthermore, the results indicate that RGO/ZnAl-LDH composite displayed a more excellent luminescence response, wide concentration range and good linear correlation to DNA than that of RGO and pure ZnAl-LDH. And the presence of LDH in the composite can effectively prevent the restacking of graphene and improve both the luminescence properties and thermal stability. The proposed method was further applied to detect the immunodeficiency virus gene (HIV), providing a new field of application of the hybrid graphene/LDH composite.

Acknowledgments

This work was supported by the National Natural Science Foundation of China (No. 201205095), the Scientic Research Foundation of Northwest A&F University (Z109021115, Z111021103 and Z111021107), the Fundamental Research Funds for the Central Universities (Z109021204), Shaanxi Province Science and Technology (No. 2013K12-03-23), State Key Laboratory of Chemo/Biosensing and Chemometrics, Hunan University (No. 2013005).

Notes and references

[a] *College of Science, Northwest A&F University, Yangling, Shaanxi, 712100, P. R. China. Fax: +86-29-87082832; Tel: +86-29-87092226; E-mail: sunsg@nwsuaf.edu.cn, hongjuanli@nwsuaf.edu.cn*

[b] *Key Laboratory of Eco-Textile, Ministry of Education, School of Textile and Clothing, Jiangnan University, 1800 Lihu Avenue Wuxi, 214122, China*

† Electronic Supplementary Information (ESI) available: The XPS wide scan spectrum and TGA curves of RGO/ZnAl-LDH composite; Luminescence spectra of $Ru(phen)_3Cl_2$ upon addition of different concentration of CT DNA; Luminescence response of $Ru(phen)_3Cl_2$ after addition of various proteins in the presence of RGO/ZnAl-LDH composite; Luminescence spectra of $Ru(phen)_3Cl_2$ upon addition of different concentration of RGO and pure ZnAl-LDH; Luminescence response of $Ru(phen)_3Cl_2$ upon addition of different concentration of DNA in the presence of RGO.

1 C. N. R. Rao, K. Biswas, K. S. Subrahmanyama and A. Govindaraj, *J. Mater. Chem.*, 2009, **19**, 2457.

2 C. N. R. Rao, A. K. Sood, K. S. Subrahmanyam and A. Govindaraj, *Angew. Chem. Int. Ed.*, 2009, **48**, 7752.

3 X. Y. Dong, L. Wang, D. Wang, C. Li and J. Jin, *Langmuir*, 2012, **28**, 293.
4 J. H. Lee, N. Park, B. G. Kim, D. S. Jung, K. Im, J. Hur and J. W. Choi, *ACS nano.*, 2013, **7**, 9366.
5 Y. Wang, Y. P. Wu, Y. Huang, F. Zhang, X. Yang, Y. F. Ma and Y. S. Chen, *J. Phys. Chem. C.*, 2011, **115**, 23192.
6 L. H. Li, X. L. Zheng, J. J. Wang, Q. Sun, and Q. Xu, *ACS Sustainable. Chem. Eng.,* 2013, **1**, 144.
7 M. Quintana, E. Vazquez and M. Prato, *Acc. Chem. Res.* 2013, **46**, 138.
8 D. Chen, L. H. Tang and J. H. Li, *Chem. Soc. Rev.,* 2010, **39**, 3157.
9 Y. X. Liu, X. C. Dong and P. Chen, *Chem. Soc. Rev.,* 2012, **41**, 2283.
10 M. Chen, Y. He, X. Chen and J. Wang, *Bioconjugate. Chem.,* 2013, **24**, 387.
11 Y. X. Ye, P. P. Wang, E. M. Dai, J. Liu, Z. F. Tian, C. H. Liang and G. S. Shao, *Phys. Chem. Chem. Phys.,* 2014, **16**, 8801.
12 S. K. Bhunia and N. R. Jana, *ACS Appl. Mater. Interfaces.,* 2011**, 3**, 3335.
13 W. L. Sun, S. Shi and T. M. Yao, *Anal. Methods*., 2011, **3**, 2472.
14 S. Stankovich, R. D. Piner, S. T. Nguyen and R. S. Ruoff, *Carbon,* 2006, **44**, 3342.
15 Y. X. Xu, H. Bai, G. W. Lu, C. Li and G. Q. Shi, *J. Am. Chem. Soc.,* 2008, **130**, 5856.
16 S. He, Z. An, M. Wei, D. G. Evans and X. Duan, *Chem. Commun.,* 2013, **49**, 5912.
17 Z. P. Liu, R. Z. Ma, M. Osada, N. Iyi, Y. Ebina, K. Takada and T. Sasaki, *J. Am. Chem. Soc.*, 2006, **128**, 4872.
18 M. J. Climent, A. Corma and S. Iborra, *Chem. Rev.*, 2010, **111**, 1072.
19 N. Baliarsingh, K. M. Parida and G. C. Pradhan, *RSC Adv*., 2013, **3**, 23865.
20 H. Hu, K. M. Xiu, S. L. Xu, W. T. Yang and F. J. Xu, *Bioconjugate. Chem.,* 2013, **24**, 968.
21 Z. An, S. Lu, L. W. Zhao and J. He, *Langmuir*, 2011, **27**, 12745.
22 Y. Wang and D. Zhang, *J. Mater. Chem. B,* 2014, **2**, 1024.
23 Z. Gao, J. Wang, Z. S. Li, W. L. Yang, B. Wang, M. J. Hou, H. Yang, Q. Liu, T. Mann, P. P. Yang , M. L. Zhang and L. H. Liu, *Chem. Mater*., 2011, **23**, 3509.
24 L. Wang, D. Wang, X. Y. Dong, Z. J. Zhang, X. F. Pei, X. J. Chen, B. Chen and J. Jin, *Chem. Commun.,* 2011, **47**, 3556.
25 L. Yan, R. Y. Li, Z. J. Li, J. K. Liu, Y. J. Fang, G. L. Wang and Z. G. Gu, *Electrochim. Acta.,* 2013, **95**, 146.
26 J. Memon, J. H. Sun, D. L. Meng, W. Ouyang, M. A. Memon, Y. Huang, S. K. Yan and J. X. Geng, *J. Mater. Chem. A,* 2014, **2**, 5060.
27 M. Latorre-Sanchez, P. Atienzar, G. Abellán, M. Puche, V. Fornés, A. Ribera and H. García, *Carbon,* 2012, **50**, 518.
28 J. L. Gunjakar, I. Y. Kim, J. M. Lee, N. S. Lee and S. J. Hwang, *Energy. Environ. Sci.*, 2013, **6**, 1008.
29 X. Y. Yuan, Y. F. Wang, J. Wang, C. Zhou, Q. Tang and X. B. Rao, *Chem. Eng. J*., 2013, **221**, 204.
30 Z. J. Huang, P. X. Wu, B. N. Gong, Y. P. Fang and N. W. Zhu, *J. Mater. Chem. A*, 2014, **2**, 5534.
31 P. A. Lay, A. M. Sargeson, H. Taube, M. H. Chou and C. Creutz, *Inorg. Synth.*, 1986, **24**, 291.
32 W. S. Hummers and R. E. Offeman, *J. Am. Chem. Soc.*, 1958, **80**, 1339.
33 Z.-H. Liu, Z. M. Wang, X. J. Yang and K. Ooi, *Langmuir*, 2002, **18**, 4926.
34 H. M. He, H. L. Kang, S. L. Ma, Y. X. Bai and X. J. Yang. *J. Colloid. Interf. Sci*., 2010, **343**, 225.
35 Z. B. Lei, L. Lu and X. S. Zhao, *Energy. Environ. Sci.,* 2012, **5**, 6391.
36 L. J. Zhang, X. J. Zhang, L. F. Shen, B. Gao, L. Hao, X. J. Lu, F. Zhang, B. Ding and C. Z. Yuan, *J. Power Sources*, 2012, **199**, 395.
37 J. Xu, S. L. Gai, F. He, N. Niu, P. Gao, Y. J. Chen and P. P. Yang, *J. Mater. Chem. A*, 2014, **2**, 1022.
38 S. Huang, G. N. Zhu, C. Zhang, W. W. Tjiu, Y. Y. Xia and T. X. Liu, *ACS Appl. Mater. Interfaces*, 2012, **4**, 2242.
39 X. B. Fan, W. C. Peng, Y. Li, X. Y. Li, S. L. Wang, G. L. Zhang and F. B. Zhang, *Adv. Mater*., 2008, **20**, 4490.
40 C. Yu, J. Yang, C. T. Zhao, X. M. Fan, G. Wang and J. S. Qiu, *Nanoscale*, 2014, **6**, 3097.
41 B. Hu, S. F. Chen, S. J. Liu, Q. S. Wu, W. T. Yao and S. H. Yu, *Chem, Eur, J*., 2008, **14**, 8928.
42 C. Xu, X. Wang and J. W. Zhu, *J. Phys. Chem. C*, 2008, **112**, 19841.
43 F. Kovanda, T. Grygar and V. Dorničcák, *Solid. State. Sci*., 2003, **5**, 1019.
44 A. B. Tossi and J. M. Kelly, *J. Photochem. Photobiol.*, 1989, **49**, 545.
45 D. Z. M. Coggan, I. S. Haworth, P. J. Bates, A. Robinson and A. Rodger, *Inorg. Chem*., 1999, **38**, 4486.
46 W. L. Sun, T. M. Yao and S. Shi, *Analyst*, 2012, **137**, 1550.
47 W. L. Sun, J. L. Yao, T. M. Yao and S. Shi, *Analyst*, 2013, 138, 421.
48 X. B. Zhang, Z. D. Wang, H. Xing, Y. Xiang anf Y. Lu, *Anal. Chem.*, 2010, **82**, 5005.